JEM Journal of Experimental Medicine

BRIEF DEFINITIVE REPORT

Epitope and HLA specificity of human TCRs against *Plasmodium falciparum* circumsporozoite protein

Hannah van Dijk[1], Ilka Wahl[1], Sara Kraker[1], Paul M. Robben[2], Sheetij Dutta[2], and Hedda Wardemann[1]

Plasmodium falciparum **malaria remains a significant global health challenge. Current vaccines elicit antibody responses against circumsporozoite protein (PfCSP) that prevent the infection of hepatocytes but offer only moderate protection. Cellular immunity has emerged as a critical component of preerythrocytic protection that might be leveraged to develop improved PfCSP vaccines. Here, we characterized the clonality, molecular features, epitope specificity, and HLA restrictions of the human PfCSP-specific CD4⁺ and CD8⁺ T cell response to vaccination with an adjuvanted PfCSP vaccine, FMP013/ALFQ. Using TCR expression cloning, we identified novel conserved CD4⁺ T cell epitopes in the PfCSP N terminus and showed that the C-terminal CS.T3 epitope was targeted by CD4⁺ and rare CD8⁺ T cells, which recognized this epitope co-receptor independently presented on a class II HLA. Our findings provide insights into the utility of these epitopes as targets for strain-transcending immunity compared with the immunodominant but highly polymorphic epitopes in the PfCSP C terminus, offering guidance for the design of improved malaria vaccines.**

Introduction

Malaria remains a significant global health issue, with *Plasmodium falciparum* (*Pf*) responsible for the most severe cases and highest mortality rates. The only available vaccines, RTS,S/AS01 and R21/Matrix-M, target *Pf* circumsporozoite protein (PfCSP), the major surface antigen of *Pf* sporozoites. Both vaccines rely primarily on the induction of anti-PfCSP antibodies that block sporozoites during their brief migration from the site of inoculation in the skin to the liver, preventing hepatocyte invasion and subsequent progression to the erythrocytic stage of infection, which causes disease (Agnandji et al., 2011; RTSS Clinical Trials Partnership, 2014; Casares et al., 2010; Datoo et al., 2022; Datoo et al., 2024). Despite inducing strong antibody responses, these vaccines provide protection, which wanes rapidly over time, particularly in high-transmission regions (Bejon et al., 2013).

T cells likely contribute to RTS,S/AS01-induced protection by providing B cell help and promoting antibody affinity maturation, as suggested by the finding that PfCSP-specific CD4⁺ T follicular helper (Tfh) cell responses were associated with improved protection (Pallikkuth et al., 2020). However, the role of T cells in preerythrocytic immunity against *Pf* goes beyond complementing humoral responses. Accumulating evidence from vaccination studies with radiation- or genetically attenuated sporozoites suggests that cellular immunity, including PfCSP-specific T cells, critically contributes to protection (Hassert et al., 2023; Oliveira et al., 2008; Rodrigues et al., 1991; Romero et al., 1989; Seder et al., 2013). In particular, CD4⁺ T cells might play a strong and multifaceted role through the production of IFN-γ, which stimulates class I and II–mediated antigen presentation, promotes the activation of cytotoxic T and natural killer cells, and mediates suppression of parasite growth in infected host cells, as well as through their direct cytolytic activity (Rénia et al., 1993; Rénia et al., 1991; Weiss et al., 1993; Romero et al., 1989). Indeed, clinical immunity induced by natural parasite exposure seems to be linked to the clonal expansion of CD4⁺ T cells with a cytotoxic phenotype against preerythrocytic antigens, including PfCSP (Nardin et al., 1989; Moreno et al., 1991; Furtado et al., 2023).

How CD8⁺ T cells against PfCSP or other *Pf* antigens contribute to malaria immunity in humans is poorly understood (Good et al., 1987; Moreno et al., 1991; Good et al., 1988; Sinigaglia et al., 1988a; Sinigaglia et al., 1988b; Moreno et al., 1993; Doolan et al., 1997; Heide et al., 2019), despite strong preclinical evidence based on adoptive T cell transfer and depletion experiments, as well as studies with T cell–deficient animals, showing that CD8⁺ T cells confer protection by eliminating infected hepatocytes via perforin-mediated lysis and IFN-γ secretion (Romero et al., 1989; Rodrigues et al., 1991; Weiss et al., 1988; Schofield et al., 1987). The assessment of CD8⁺ T cell responses to *Pf* in humans is hampered by the relative weakness and fast

[1]B Cell Immunology, German Cancer Research Center, Heidelberg, Germany; [2]Biologics Research and Development Branch, Center for Infectious Diseases Research, Walter Reed Army Institute of Research, Silver Spring, MD, USA.

Correspondence to Hedda Wardemann: h.wardemann@dkfz-heidelberg.de.

decline of CD8⁺ responses in circulation after vaccination and their tissue residency at the site of infection, i.e., the liver after natural or immunization-mediated exposure to sporozoites (Weiss and Jiang, 2012; Trimnell et al., 2009; Schofield et al., 1987; Hoffman et al., 1989).

Despite the evidence that PfCSP-specific CD4⁺ and potentially also CD8⁺ T cells play a role in protection from malaria, little is known about the molecular characteristics of TCRs that mediate PfCSP binding to inform the design of vaccines with the potential to mediate more potent protection. PfCSP consists of a central repeat region flanked by a short junctional peptide, which connects the repeat to the N-terminal domain and a C-terminal domain. Bulk cell analyses have shown that T cell epitopes are distributed across the junctional peptide and N- and C-terminal domains, but are absent from the central repeat region. CD4⁺ T cells mainly target Th2R and T*, two epitopes in the C-terminal α-thrombospondin type-I repeat domain, with weaker responses against the CS.T3 epitope in the C terminus and the T1 epitope in the N-terminal junction (Moreno et al., 1993; Moreno et al., 1991; Wahl et al., 2022b; Good et al., 1987). Differences in immunogenicity among these epitopes are linked to HLA restrictions and differences in sequence conservation of the target peptides with stronger immune responses to the polymorphic epitopes Th2R and T* that are presented on diverse HLA alleles, compared with the more conserved CS.T3 and T1 epitopes with stronger HLA restrictions (Good et al., 1988; Schwenk et al., 2011).

The polymorphic nature of the immunodominant C-terminal PfCSP epitopes poses a challenge to vaccine development, as it limits cross-strain immunity (Zeeshan et al., 2012; de la Cruz et al., 1988; Neafsey et al., 2015). A detailed understanding of epitope-specific T cell responses, including their HLA restriction and TCR usage, is critical to overcome these limitations and guiding the design of next-generation malaria vaccines that elicit robust, strain-transcending T cell and antibody responses for broad and efficacious protection (Beura et al., 2018).

We have recently characterized the PfCSP-specific circulating Tfh cell response to irradiated sporozoite vaccination at single-cell level, which identified highly strain-specific TCRs against supertopes in the polymorphic Th2R/T* region (Wahl et al., 2022b). In this study, we analyzed the peripheral PfCSP-specific CD4⁺ and CD8⁺ T cell responses in malaria-naive individuals vaccinated with Falciparum Malaria Protein 013 (FMP013), a nearly full-length recombinant PfCSP adjuvanted in Army Liposome Formulation containing QS21 (ALFQ), which induced strong antibody responses against the C terminus and gradually weaker responses against the central repeat and N-terminal domains in a recent phase I study (Hutter et al., 2022). Using single-cell TCR sequencing, expression cloning, and functional assays, we identified novel and conserved epitopes within the N- and C-terminal domains. We further characterized the gene usage, HLA restriction, and functional properties of these TCRs, revealing a highly polyclonal, donor-specific CD4⁺ T cell repertoire dominated by responses to C-CSP. Our findings also provide new insights into the rare CD8⁺ T cell responses against PfCSP, including a co-receptor–independent TCR targeting a shared CD4⁺/CD8⁺ epitope presented in an HLA-DP–restricted manner. These data expand our understanding of PfCSP-specific T cell immunity and highlight CS.T3 as an important target for the development of broadly protective malaria vaccines.

Results and discussion

CD4⁺ T cell response to repeated PfCSP vaccination

To characterize the human CD4⁺ T cell response to PfCSP, we isolated peripheral blood mononuclear cells (PBMCs) from seven malaria-naive individuals (F1–5, F7, F9) isolated 4 wk after vaccination with two doses of recombinant Pf3D7 strain-based PfCSP vaccine FMP013 in ALFQ, an adjuvant that also contains the synthetic monophosphoryl lipid A derivative analog 3D-PHAD (Fig. 1 A; Hutter et al., 2022). To identify PfCSP-reactive T cells, we first stimulated PBMC samples from two donors (F7 and F9) with pools of overlapping peptides covering the complete immunogen PfCSP aa sequence (3D7 aa Tyr_{26}–Ser_{383}; Fig. 1 B). Flow cytometric analyses showed an increase in the number of activated CD4⁺ T cells expressing the activation markers CD25 and OX40 compared with unstimulated control cultures from both donors demonstrating that antigen-reactive CD4⁺ T cells were circulating in blood 28 days after the second FMP013/ALFQ vaccination. To determine the clonal composition of the activated T cells, we isolated single CD4⁺CD25⁺OX40⁺ T cells from the stimulated cultures by indexed flow cytometric cell sorting and amplified and sequenced their paired *TRA* and *TRB* genes (Fig. S1 A). Only about half of the sequences (47% in F7 and 53% in F9) were obtained from lowly expanded clones encoded by diverse V segments, reflecting the highly polyclonal nature of the anti-FMP013 response in both individuals (Fig. 1 C).

To distinguish the response to the individual PfCSP subdomains, we stimulated PBMCs from the other five donors with peptide pools covering either the N terminus, junction region, and repeat domain (N-CSP) or the complete C terminus (C-CSP; Fig. 1 D). T cells from all individuals responded to stimulation with C-CSP peptides, whereas cultures from only three of the five donors responded to N-CSP peptide stimulation. TCR gene sequencing of the activated cells from the two donors with the strongest N- and C-CSP responses showed that the degree of clonal expansion was lower after N-CSP (36% in F3 and 7% in F4) compared with C-CSP peptide pool stimulation (61% in F3 and 27% in F4), in line with previous reports demonstrating the immunodominance of C-terminal compared with N-terminal and junction epitopes (Moreno et al., 1991; Reece et al., 2004). The absence of any clonal overlap between the cultures and differences in *TRAV* and *TRBV* gene enrichment between cultures from different donors after N- and C-CSP peptide pool stimulation and compared with unstimulated control cells from the same individuals indicated that the cells expanded peptide and HLA specifically and reflect the privacy of the PfCSP-specific response (*TRAV*: *29-DV5*, *17-1*, *8-6*, *41-1*; *TRBV*: *30-1*, *3-1*, *12-3*, *20-1*, *6-1*; Fig. 1 F and Fig. S1 B). In summary, FMP013/ALFQ vaccination induced polyclonal CD4⁺ responses with diverse TCRs against the PfCSP C terminus in all donors, whereas responses against the N terminus, junction, and repeat domain were induced in only a few individuals.

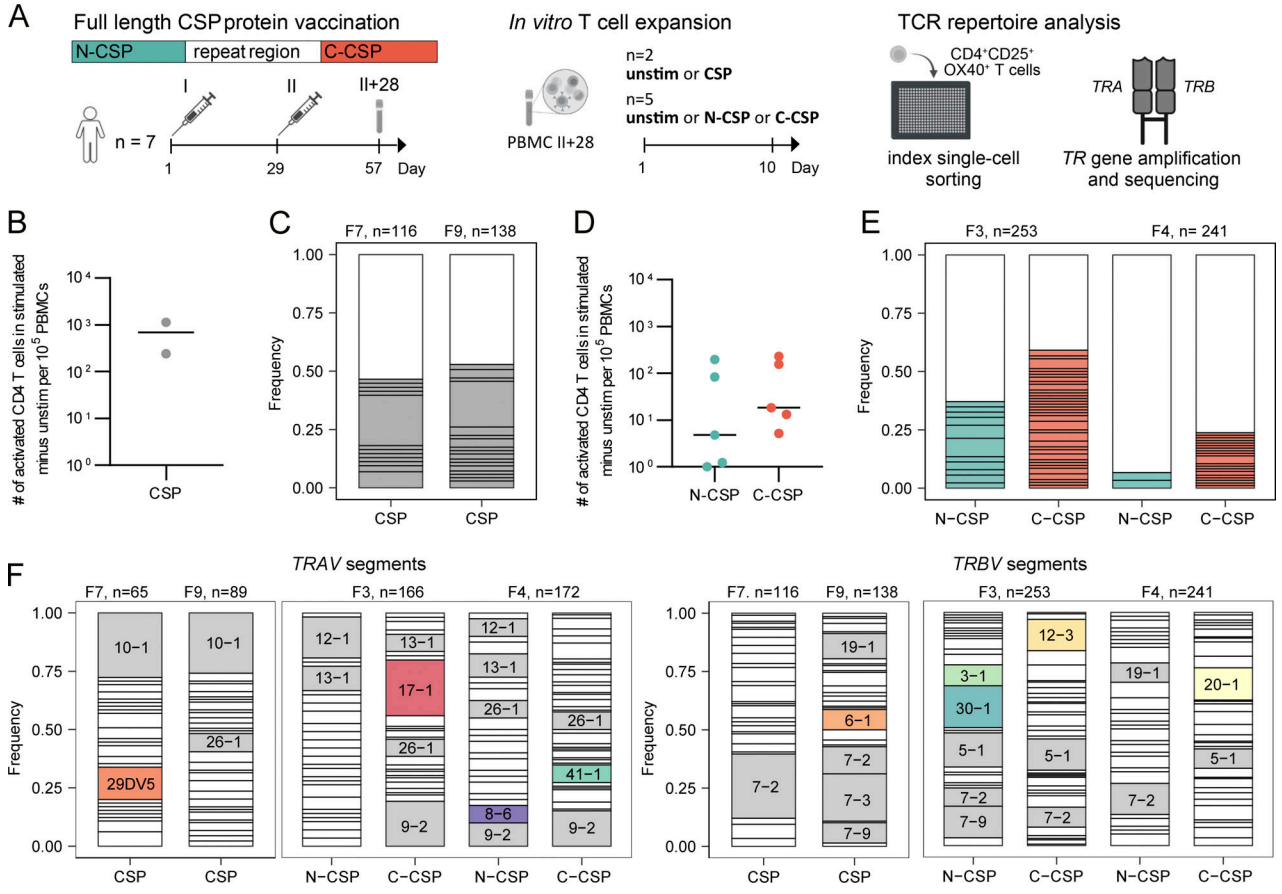

Figure 1. **Vaccination-induced polyclonal CD4⁺ T cells targeting the PfCSP N and C terminus. (A)** Schematic overview of the sample collection, in vitro stimulation, and single-cell isolation strategy. PBMC samples collected 28 days after two FMP013/ALFQ vaccine doses (II+28) were left untreated or stimulated with peptide pools covering the complete FMP013 aa sequence (CSP), the FMP013 N terminus, junction, and repeat domain (N-CSP), or the FMP013 C terminus (C-CSP). Indexed flow cytometric single-cell sorting was performed 10 days later. **(B and D)** Number of activated ($CD25^+OX40^+$) $CD4^+$ T cells after in vitro peptide pool stimulation compared with unstimulated control cells from the same individuals. Each symbol represents a volunteer. **(C and E)** Clonal composition and *TRAV* and *TRBV* gene segment usage of single activated $CD4^+$ T cells after CSP (C) or N-CSP and C-CSP (E) peptide pool stimulation of samples from the indicated donors. Individual expanded clones are shown in color, and all non-expanded clones are shown in white. **(F)** *TRAV* and *TRBV* gene usage after in vitro stimulation, *TRAV* and *TRBV* gene segments (>7%) enriched in activated cells isolated from peptide-stimulated cultures are labelled, and nonoverlapping segments highlighted in color. B–F represent data from one experiment.

Polyclonal PfCSP-specific CD4⁺ T cells target N-terminal, junction, and C-terminal epitopes

To determine whether the activated and expanded T cell clones were PfCSP-reactive, we cloned the TCRs of 66 selected clones, including several with enriched gene segments after the stimulation, and expressed them in $CD4^+$-positive TCR-deficient Jurkat76 cells (Fig. S1 C and Table S1). More than half (53%, 35/66) of the T cell lines secreted IL-2 after in vitro co-culture with autologous B cells pulsed with the C-CSP or N-CSP peptide pools (Fig. 2 A). Two thirds (69%, 24/35) showed specificity for C-CSP peptides, whereas one third (31%, 11/35) reacted exclusively to N-CSP peptides (Fig. 2 B). Stimulation of these clones with individual peptides identified their target epitopes (Fig. 2, C and D). The N-CSP–specific TCRs reacted to two novel, highly conserved epitopes covering aa 61–75 (4/11) and 81–95 (1/11), hereafter referred to as CSP61 and CSP81, respectively, or to the T1 epitope in the N-terminal junction (6/11) but not to the repeat (Fig. 2, C and D). The C-CSP–reactive TCRs recognized peptides covering the known polymorphic Th2R (peptide 315–319; 15/24) and T* epitopes (peptide 319–337; 2/24) as well as CS.T3 (peptide 367–381; 7/24) (Fig. 2 C; Sinigaglia et al., 1988b; Good et al., 1988; Guttinger et al., 1988). Although the PfCSP-reactive TCRs were encoded by diverse *TRAV* and *TRBV* combinations, we observed several associations between epitope specificity and V gene usage (Fig. 2, E and F). Specifically, T1 binding was linked to *TRBV30-1* usage as previously reported (Wahl et al., 2022b), whereas the majority of Th2R and CS.T3 reactive TCRs were encoded by *TRAV17-1* and *TRBV20-1*, respectively (Fig. 2 F). In summary, we identified $CD4^+$ T cell–associated TCRs against epitopes in the PfCSP C and N terminus, including two novel N-terminal epitopes, and defined TCR gene usage patterns associated with reactivity against several of these targets.

PfCSP-specific TCRs are restricted to HLA alleles with variable prevalence

To determine the HLA restriction of the peptide-specific TCRs, we performed the co-culture stimulation assay with autologous

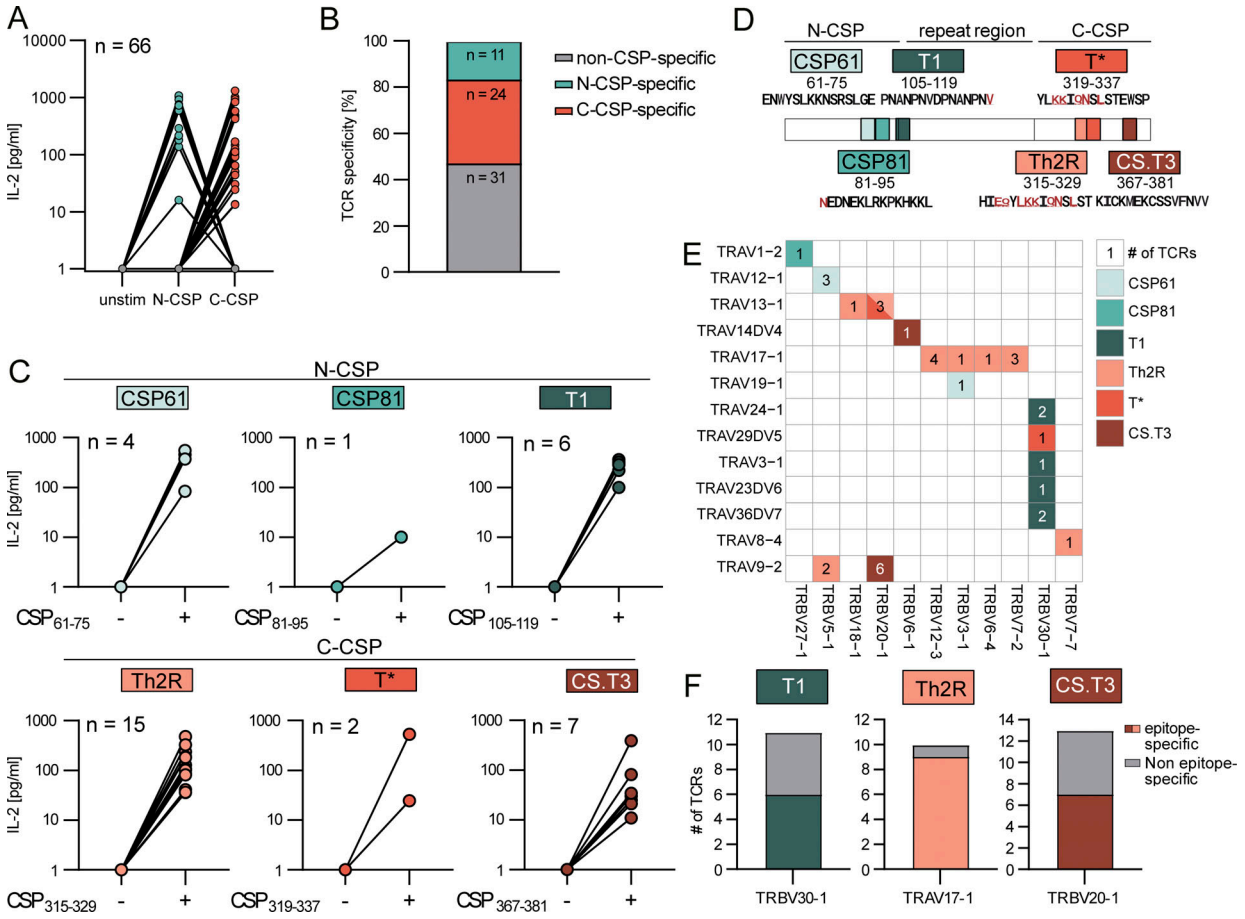

Figure 2. **PfCSP-specific CD4⁺ T cells target three N-CSP and three C-CSP epitopes.** Transgenic CD4⁺ Jurkat76 T cell lines expressing TCRs from T cells with an activated phenotype after stimulation of PBMCs with N- or C-CSP peptide pools (donors F3, F4, F7, and F9) were generated. **(A)** IL-2 concentrations as quantified by ELISA in supernatants of T cell lines (n = 66) co-cultured with autologous B cells pulsed with N-CSP or C-CSP peptide pools or with non-peptide–pulsed autologous B cells (unstim). Color coded by specificity (gray: non-CSP specific, turquoise: N-CSP specific, and orange: C-CSP specific). **(B)** Frequency of N- and C-CSP–reactive and nonreactive TCRs. **(C)** IL-2 concentrations as quantified by ELISA in supernatants of T cell lines co-cultured with autologous B cells pulsed with the indicated peptides (+) or left unstimulated (–). n indicates the number of tested T cell lines. **(D)** Schematic map of the identified target epitopes and aa positions within PfCSP. Sequence diversity of TCR epitopes among 481 PfCSP sequences isolated from seven geographic regions published by Tanabe et al. (2013), and polymorphic aas are highlighted in red. **(E)** *TRAV* and *TRBV* usage and number of individual TCRs with the indicated epitope specificity. **(F)** Number of epitope-specific TCRs among all cloned and tested TCRs with the indicated V segments. **(A–C, E, and F)** Data from one out of two independent experiments are shown.

B cells in the presence of HLA-DR–, DQ-, and DP-blocking antibodies (Fig. 3 A). The anti-HLA-DR antibody exclusively blocked the activation of all T cell lines expressing CSP61-, CSP81-, Th2R-, and CS.T3-specific TCRs, whereas the activation of T1-specific T cell lines was blocked specifically by anti-HLA-DQ. In contrast, activation of the T*-specific TCRs was strongly inhibited by HLA-DR– or HLA-DQ–blocking antibodies.

Next, to define or infer the HLA allele specificity of all TCRs, we performed heterologous stimulation experiments of the T cell lines with peptide-pulsed B cells from donors that shared only a single or no HLA allele (Fig. 3 B). All TCRs that targeted N-terminal epitopes (CSP61, CSP81, and T1) recognized their specific target peptide in the context of a single HLA allele (DRB1*13:02, DRB4*01:03, and DQB1*06:03, respectively). In contrast, the TCRs with reactivity against the PfCSP C terminus were restricted to two alleles. The two Th2R-specific TCRs were activated by peptides presented in the context of DRB1*13:02 and DRB1*10:01, whereas the two T*-specific TCRs were restricted to DQB1*02:02 and DRB1*13:02, and the CS.T3-specific TCRs recognized their epitope on DRB1*10:01 and DRB4*01:03. The number of individuals that expressed the above alleles or alleles that we previously reported to present Th2R peptides (DRB1*07:01 or DRB1*15:01 [Wahl et al., 2022b]) varied strongly among the donors analyzed in this study (Fig. 3 C). The majority of donors expressed HLA alleles that induced T cell responses against the polymorphic Th2R and T* epitopes (10/15 and 7/15, respectively), reflecting the high abundance of TCRs with specificity for peptides covering this region (Fig. 3 D). Alleles presenting the conserved CS.T3 and N-terminal peptides were less frequent, in line with the lower frequency of TCRs with these specificities (Fig. 2). In summary, we identified novel and abundant HLA alleles presenting the immunodominant Th2R and T* peptides and determined the allele context for TCRs against novel, conserved CD4⁺ T cell epitopes in the PfCSP N

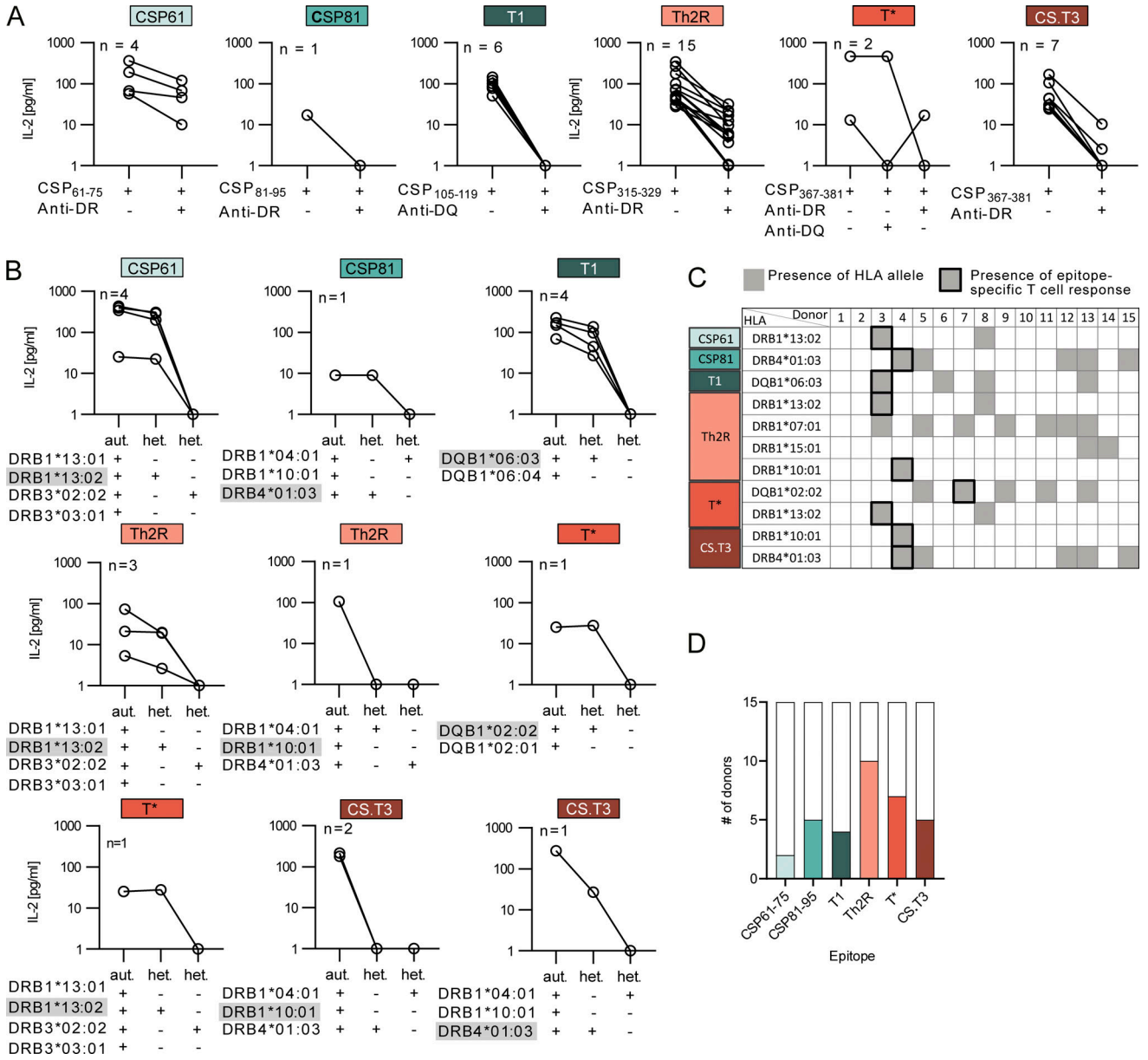

Figure 3. **PfCSP epitopes are presented on HLA alleles with variable prevalence. (A)** IL-2 concentrations as measured by ELISA in supernatants of TCR-transgenic CD4⁺ Jurkat76 T cells co-cultured with autologous B cells pulsed with the indicated peptides in the presence (+) or absence (–) of the indicated locus-specific HLA-blocking antibodies. **(B)** IL-2 concentrations as measured by ELISA in supernatant of TCR-transgenic CD4⁺ Jurkat76 T cells co-cultured with peptide-pulsed autologous (aut.) or heterologous (het.) B cells that share one (+) or no (–) locus-specific HLA allele with the respective autologous B cells. Epitope-presenting HLA alleles were determined (activation observed in co-cultures with heterologous B cells expressing a single share allele) or inferred (lack of activation in heterologous B cells with one shared allele) and are highlighted in gray. **(C)** HLA alleles presenting the indicated PfCSP epitopes in the 15 donors described in this study (DRB1*13:02, DRB1*04:03, DQB1*06:03, DRB1*10:01, and DQB1*02:02) or previously (DRB1*07:01 and DRB1*15:01 [Wahl et al., 2022b]). Gray shading indicates the presence of an allele. Black frames indicate epitope-specific CD4⁺ T cell responses as determined in A. **(D)** Frequency of donors with HLA alleles shown to present the indicated epitopes. **(A and B)** *n* indicates the number of tested T cell lines. One out of two independent experiments is shown.

terminus (CSP61 and CSP81) and the conserved CS.T3 epitope in the C terminus.

N- and C-terminal PfCSP peptides are presented on diverse HLA class I alleles

Several of the CD4⁺ T cell epitopes, including the newly identified, conserved CSP61 and CSP81 epitopes and CS.T3, have previously been associated with HLA class I–restricted CD8⁺ T cell responses (Wang et al., 1998; González et al., 2000; Doolan et al., 1991; Sedegah et al., 2013), which prompted us to investigate the CD8⁺ T cell response against PfCSP in the same vaccinated individuals. We first used NetMHCIpan4.0 (Reynisson et al., 2020), a computational peptide-MHC prediction algorithm, to estimate the binding strength of the different HLA class I molecules expressed by the donors in our study to peptides covering the complete FMP013 aa sequence (Fig. 4 A).

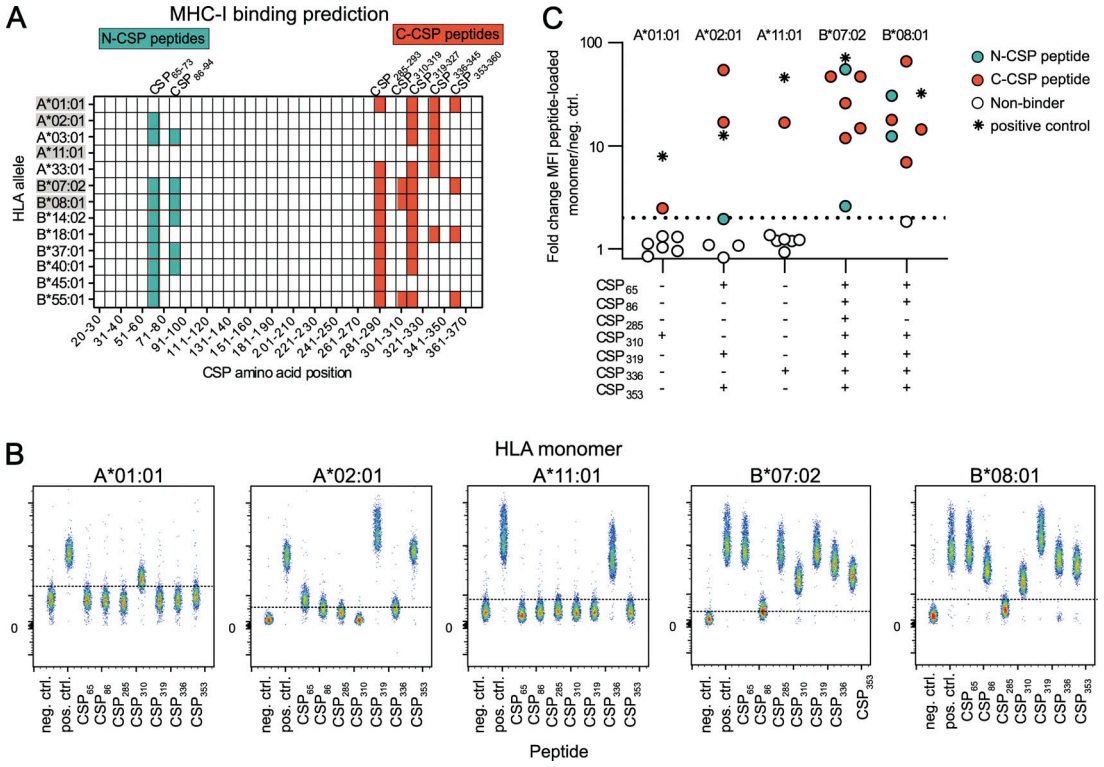

Figure 4. **N- and C-terminal peptides bind HLA class I alleles promiscuously. (A)** Peptide-binding prediction of PfCSP peptides to HLA-A and HLA-B alleles of five vaccinated donors by NetMHCpan4.1 tool. Predicted peptides (9–11mer length, EL-rank threshold below 7) within the FMP013 aa sequence (position 20–380) are highlighted in color and shown within starting position ranges of 10 aa. **(B and C)** Binding of seven predicted PfCSP peptides to five HLA monomer. **(B)** FACS plot of β-microglobulin–stained monomers loaded with individual peptides compared with allele-specific negative and positive controls. **(C)** Fold change in MFI of peptide-loaded monomers relative to allele-specific negative controls. **(B and C)** represent one experiment. MFI, median fluorescence intensity.

Seven PfCSP peptides, two N-terminal peptides ($CSP_{65–73}$ and $CSP_{86–94}$) and five C-terminal peptides ($CSP_{285–293}$, $CSP_{310–319}$, $CSP_{319–327}$, $CSP_{336–345}$, and $CSP_{353–360}$) were predicted to bind strongly to three or more of the 13 HLA-A and B alleles that were detected in our cohort. For five HLA alleles with high prevalence (HLA-A*01:01, HLA-A*02:01, and HLA-A*11:01) or high number of strong predicted binders (HLA-B*07:02 and HLA-B*08:01), peptide binding was confirmed using HLA monomers loaded with the predicted N-terminal or C-terminal peptides (Fig. 4 B). In line with the binding predictions, HLA-B*07:02 and HLA*B08:01 bound more peptides with higher apparent affinity than the more frequent HLA-A alleles A*01:01, A*02:01, and A*11:01 (Fig. 4 C). The detection of HLA-A and B alleles that can present N- and C-terminal peptides prompted us to assess whether we could detect anti-PfCSP $CD8^+$ responses.

To identify $CD8^+$ T cells that had responded to the vaccination, we isolated single $CD8^+$ T cells with an activated phenotype based on the expression of PD-1, ICOS, CXCR5, and CD137 from PBMCs of five donors expressing at least one HLA allele with confirmed PfCSP peptide binding before and after vaccination (Fig. S1, D and E). TCR gene amplification and sequencing identified high frequencies of large persistent clones whose TCR genes showed similarity in TCR beta chain CDR3 sequences with those of TCRs with specificity against common viruses such as CMV, EBV, influenza, but also hepatitis B virus, SARS-CoV, and yellow fever virus, demonstrating that the activated $CD8^+$ T cell repertoire under steady-state conditions is dominated by cells expressing TCR genes associated with antiviral reactivity, which persist after vaccination (Fig. S1, F and G). Expression cloning of 66 TCRs from cells that lacked these sequence features and were not detected before the vaccination failed to identify PfCSP-reactive clones, demonstrating the relative scarcity of PfCSP-reactive $CD8^+$ compared with antiviral T cells with an activated phenotype (Fig. S1 H).

Rare PfCSP-specific $CD8^+$ T cells target an HLA class II–restricted C-terminal epitope

To enrich for PfCSP-reactive $CD8^+$ T cells, we performed in vitro stimulation experiments and assessed the frequency of activated $CD8^+$ T cells ($CD69^+CD137^+$) analogous to the strategy successfully used for the enrichment of PfCSP-reactive $CD4^+$ T cells (Fig. S1 A). We initially stimulated PBMCs from two donors with peptides covering the complete PfCSP sequence, which led to strong activation and low levels of $CD8^+$ T cell clonal expansion (Fig. 5 A and Fig. S2 A). Stimulation of PBMCs from five additional donors with the separate peptide pools against the PfCSP subdomains induced C-CSP responses in four but N-CSP responses in only one donor (Fig. 5 A). In contrast to the N- or C-CSP–specific clonal expansion observed for $CD4^+$ T cell responses (Fig. 1, C and E), the majority of expanded $CD8^+$ T cell

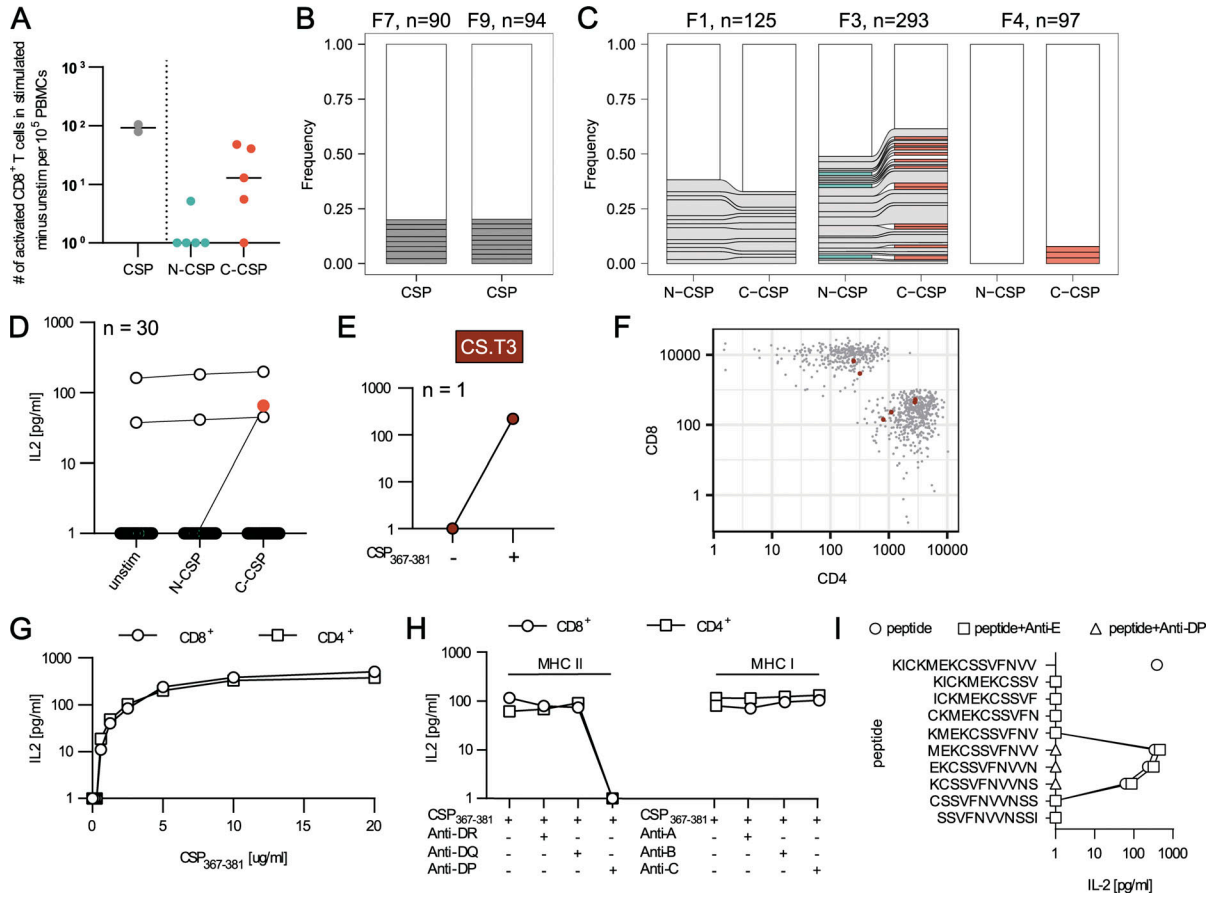

Figure 5. **Rare PfCSP-specific CD8⁺ T cells target an HLA class II–restricted C-terminal epitope co-receptor independently. (A)** Number of activated (CD69⁺CD137⁺) CD8⁺ T cells from seven vaccinated donors (F7+F9, F1–5) after CSP, N-CSP, or C-CSP peptide pool-mediated in vitro stimulation compared with unstimulated control cells from the same individuals. **(B and C)** Activated T cells were index single-cell sorted for paired *TRA* and *TRB* gene amplification and sequencing. Clonal composition of activated CD8⁺ T cells after CSP, N-CSP, or C-CSP peptide stimulation of samples from the indicated donors (F7, F9; F1, F3, F4). Expanded clones are shown in color, and non-expanded clones are combined in white. Shared clones across separate expansion cultures are connected by ribbon. **(D)** Transgenic CD8⁺ Jurkat76 T cell lines were generated expressing TCRs from CD8⁺ T cells with an activated phenotype after stimulation of PBMCs with N- or C-CSP peptide pools. All monoclonal T cell lines were co-cultured with autologous B cells pulsed with N-CSP or C-CSP peptide pools or with non-peptide–pulsed autologous B cells (unstimulated control). For each T cell line, the IL-2 concentrations in culture supernatants as measure for TCR-mediated activation were quantified by ELISA (individual dots). **(E)** IL-2 concentrations as quantified by ELISA in supernatants of C-CSP reactive T cell line co-cultured with autologous B cells pulsed with the CS.T3 peptide ($CSP_{367-381}$) (+) or left unstimulated (–). **(F)** CD4/CD8 phenotype of single-cell sorted activated T cells in the expansion culture. Clonally related cells ($n = 6$) among the PfCSP-reactive T cell clone are highlighted in red. **(G)** IL-2 concentrations in supernatants of TCR-transgenic CD4⁺ or CD8⁺ Jurkat76 T cells co-cultured with $CSP_{367-381}$ peptide-pulsed autologous B cells at the indicated peptide concentrations. **(H)** IL-2 concentrations in supernatants of TCR-transgenic CD4⁺ or CD8⁺ Jurkat76 T cells co-cultured with peptide-pulsed autologous B cells in the presence or absence of the indicated locus-specific HLA-blocking antibodies. **(I)** IL-2 concentrations in supernatants of TCR-transgenic CD8⁺ Jurkat76 T cells co-cultured with peptide-pulsed autologous B cells in the absence or presence of HLA-E or HLA-DP-specific HLA-blocking antibodies. A–C and F represent one experiment. **(D, E, G, H, and I)** One out of two independent experiments is shown.

clones (80%, F1, 100% 13/13, F3, 62% 23/37) were detected across both peptide stimulation conditions indicative of bystander activation (Fig. 5 C). We therefore selected 30 expanded clones with V segments that were enriched uniquely after N- or C-CSP peptide pool stimulation without overlap between the two conditions for TCR expression cloning into CD8⁺ Jurkat76 T cells. Co-cultivation of the TCR-transgenic cell lines with N-CSP and C-CSP peptide pool pulsed or unstimulated autologous B cells identified only one PfCSP-reactive clone with C-CSP specificity, whereas two clones responded under all conditions, most likely because they recognized abundant EBV peptides presented after the B cell immortalization (Fig. 5 D and Table S1).

Stimulation with single peptide-pulsed autologous B cells identified peptide 367–381, representing CS.T3 as cognate epitope of the C-CSP–reactive CD8⁺ TCR (Fig. 5 E). Because our data showed that the CS.T3 epitope was also recognized by CD4⁺ T cells (Fig. 2), we assessed the phenotype of the cell from which the TCR had been cloned. The CS.T3-reactive CD8⁺ T cell belonged to a larger clone with identical CDR3 nucleotide sequence of six members, including four with a CD4⁺ phenotype, sorted from CD4⁺-activated cells, suggesting that this TCR binds the CS.T3 epitope co-receptor independently (Fig. 5 F). Indeed, when we expressed the TCR in CD4⁺ Jurkat76 T cells, we observed the same concentration-dependent activation kinetic after CS.T3 peptide stimulation as with the CD8⁺ Jurkat76 T cells,

demonstrating the co-receptor independence of this TCR (Fig. 5 G). Surprisingly, the use of anti-HLA–blocking antibodies showed that the activation of both cell lines was blocked by the addition of an HLA-DP–specific antibody demonstrating that the TCR recognized the peptide in the context of class II even when expressed by CD8⁺ T cells (Fig. 5 H). Using an HLA-E–specific blocking antibody, we excluded the possibility that recognition of the CS.T3 peptide 367–381 was HLA-E dependent, although the peptide was predicted to be a strong HLA-E binder (Fig. 5 I). Through HLA-typing and peptide-binding predictions, we linked CS.T3 targeting to two non-shared HLA-DP alleles, HLA-DPB*10:01 and HLA-DPB*17:01, with high predicted binding to the core peptide EKCSSVFNVVN. The TCR of the CS.T3-reactive clone with mixed CD8⁺ and CD4⁺ phenotype was encoded by *TRBV7-2* and *TRAV36DV7*, and thus showed no similarity with the CS.T3-specific TCRs of cells with only a CD4⁺ phenotype, which were frequently encoded by *TRBV20-1* (Fig. 2), adding to the uniqueness of the co-receptor–independent TCR.

In summary, although we were unable to identify class I–restricted TCRs with reactivity against any of the predicted PfCSP peptides with strong binding to diverse HLA-A and HLA-B molecules, we identified rare CD8⁺ T cells with specificity for CS.T3 that recognized their target peptide co-receptor independently when presented on HLA-DP, just like their CD4⁺ clonal relatives.

Previous studies on T cell responses to PfCSP primarily focused on highly immunogenic but polymorphic CD4⁺ T cell epitopes, leaving subdominant epitopes with high sequence conservation largely uncharacterized (Moreno et al., 1993). Using human blood samples from FMP013/ALFQ vaccines, we detected novel conserved epitopes in the PfCSP N and C terminus, which had not been identified after RTS,S or irradiated sporozoite vaccination (Lalvani et al., 1999; Wahl et al., 2022b). Although in vitro stimulation enabled the amplification and detection of T cell responses to less immunogenic epitopes, the high degree of non-PfCSP–specific bystander activation and substantial overlap between CD4⁺ and CD8⁺ T cell epitopes highlights the need for functional validation at monoclonal TCR level or at least subset-specific T cell depletion (Oberhardt et al., 2021; Gondré-Lewis et al., 2023; Montes et al., 2005; Reiss et al., 2017).

The stronger cellular response and higher frequency of C-CSP compared with N-CSP peptide pool-reactive T cells in all donors confirms the immunodominance of the C over the N terminus and junction region, similar to responses that we observed with irradiated sporozoite vaccination (Wahl et al., 2022b). Nonetheless, FMP013/ALFQ facilitated responses against novel N-terminal epitopes (CSP61 and CSP81). Whether the PfCSP N terminus may represent an underappreciated target for T cell–based immunity requires confirmation. Our previous study failed to identify N terminus–reactive T cells in individuals vaccinated with high doses of irradiated sporozoites, potentially linked to the proteolytic cleavage of the PfCSP N terminus on the parasite surface or the fact that we did not enrich for N terminus reactivity by in vitro stimulation (Coppi et al., 2011; Singer et al., 2024).

While FMP013/ALFQ vaccination induced responses against all reported PfCSP CD4⁺ T cell epitopes, the CD8⁺ T cell response was restricted to CS.T3, contrasting the high number of CD8⁺ epitopes across all subdomains that have been reported in the past and expectations based on mouse studies (Heide et al., 2019). This discrepancy might be explained by the fact that the historic PfCSP CD8⁺ T cell epitope and HLA restrictions data originate from bulk cell stimulation and peptide-binding predictions or in vitro peptide-binding assays that were never confirmed at monoclonal TCR level (Sedegah et al., 2013; Heide et al., 2019). Indeed, our own data indicate that even dextramer-based stainings can be misleading, as we were unable to confirm the TCR specificity of dextramer-reactive T cells enriched in cultures following in vitro stimulation with peptides that had shown confirmed dextramer binding—presumably due to low peptide compared with HLA reactivity (Fig. S2, B–E). Alternatively, and not mutually exclusive, PfCSP as delivered in the FMP013/ALFQ vaccine may not effectively prime CD8⁺ T cells in humans compared with sporozoite immunization or natural *Pf* infection. Although previous studies on PfCSP-based vaccines, such as RTS,S/AS01 and R21/Matrix-M, have demonstrated the induction of PfCSP-specific T cells and linked PfCSP-specific Tfh cells to enhanced protection, the role of cellular immunity in preerythrocytic protection beyond complementing humoral responses remains unclear (Pallikkuth et al., 2020). Nonetheless, we identified a rare CS.T3-specific CD8⁺ T cell clone, suggesting that this epitope is a relevant target of the cytotoxic anti-PfCSP response.

Our analysis revealed associations between TCR V-gene usage and epitope specificity, including the strong enrichment of *TRBV30-1* in T1-specific TCRs and *TRBV20-1* in CS.T3-specific TCRs. These findings align with our previous report of conserved TCR motifs linked to PfCSP-specific responses and together might provide an opportunity to identify T cell responses against defined epitopes by sequence analysis alone (Wahl et al., 2022b). Furthermore, our data illustrate the positive correlation between the diversity of HLAs that present a given peptide and the strength of the T cell response against this target. The fact that the highly immunogenic Th2R and T* epitopes lie in the most polymorphic regions of PfCSP likely reflect the immune pressure that cellular responses exert on natural parasite populations. The conserved nature of the weaker immunogenic CSP61, CSP81, T1, and CS.T3 epitopes enhances their potential utility as vaccine targets for inducing strain-transcending immunity, addressing a critical limitation of RTS,S/AS01 (and potentially also R21/Matrix-M), which exhibits reduced efficacy against natural parasite populations with little sequence homology to the 3D7-derived vaccine C-terminal domain (Neafsey et al., 2015). Nevertheless, their stronger HLA restriction poses a challenge to the development of improved vaccine candidates that will be capable of inducing broad cellular anti-PfCSP immune responses.

The most promising seems to be CS.T3, which binds to diverse HLA alleles (Sinigaglia et al., 1988b), was targeted by CD4⁺ and CD8⁺ T cells, and is associated with protective T cell responses to natural infections (Reece et al., 2004). The high degree of sequence conservation likely reflects a yet unknown critical function of this PfCSP epitope for parasite development in the mosquito vector or human host. The low number of CS.T3

responders after RTS,S/AS01 and irradiated sporozoite vaccination (Lalvani et al., 1999; Wahl et al., 2022b) and scarcity of the CS.T3-presenting HLA-DRB*10 allele in this study highlight the challenge of inducing CS.T3-specific CD4+ T cell responses by vaccination. The unique anti-CS.T3 T cell clone with CD4+ and CD8+ members that we identified recognized its peptide exclusively in the context of HLA-DP, indicating a dominant role of CD4+ T cells in CS.T3 targeting. The co-receptor–independent activation suggests high TCR affinity to compensate for the lack of co-receptor signaling in the context of CD8+ T cells (Laugel et al., 2007), potentially enhancing cellular responses through the simultaneous activation of functionally diverse CD4+ and CD8+ T cell subsets (Davari et al., 2021). This unique TCR configuration highlights the potential for unconventional PfCSP-specific T cell responses that may bypass classical MHC restrictions.

Recent findings highlight the potential of CD4+ T cells to exhibit cytotoxic activity and produce high levels of IFN-γ (Burel et al., 2016; Furtado et al., 2023), challenging the traditional association of cytotoxic function with CD8+ T cells. While this study characterized the T cell response to FMP013/ALFQ vaccination, recently advancing alternative vaccine strategies, including genetically attenuated sporozoite vaccination and nucleic acid–based vaccines, might lead to the induction of higher antigen-specific T cell frequencies through improved MHC presentation and T cell priming (Hoffman and Doolan, 2000; Wang et al., 1998; Lamers et al., 2024). It will be crucial to evaluate those T cell responses at monoclonal TCR level to gain additional information on gene sequence features associated with HLA and peptide binding and obtain training sets for algorithms that reliably predict T cell responses against PfCSP epitopes in malaria vaccine target populations. Although conserved PfCSP epitopes are restricted to less prevalent HLA alleles, combinations of epitopes that are presented on several low prevalent HLA alleles can reach population-wide coverage, lowering the risk for T cell–mediated escape (Tsuji and Zavala, 2001).

This study has several limitations. First, the analysis was restricted to malaria-naive individuals in the U.S., and it remains unclear how prior exposure to *Pf* and HLA haplotype diversity in individuals living in malaria endemic or other infections might influence PfCSP-specific T cell responses. Second, while we identified several conserved epitopes and their HLA restrictions, functional validation of these responses in vivo and their correlation with protection remain to be established. Finally, we cannot exclude that the scarcity of PfCSP-specific CD8+ T cells identified in this study might be partly associated with non-optimal stimulation conditions in the in vitro assay due to the use of 15mer instead of shorter peptides. The data highlight the need for targeted studies aiming to explore factors that limit the induction of anti-PfCSP CD8+ T cells and the potential role of alternative PfCSP delivery platforms.

In summary, our study provides a detailed molecular characterization of PfCSP-specific T cell responses induced by FMP013/ALFQ vaccination, providing a foundation for the rational design of vaccines that elicit robust, strain-transcending T cell responses. Future studies should focus on validating these findings in larger and more diverse cohorts and exploring strategies to enhance PfCSP-specific T cell priming for improved preerythrocytic immunity.

Materials and methods

Human FMP013 vaccine trial

The FMP013 vaccination trial (ClinicalTrials.gov identifier NCT04268420) was conducted in accordance with all applicable USA Federal and Department of Defense human research protections requirements under Food and Drug Administration Investigational New Drug as previously reported (Hutter et al., 2022). PBMC samples isolated 7 days before the first, 28 days after the second, and 14 days after the third immunization were analyzed upon approval by the ethics committee of the medical faculty of the University Heidelberg (number: S-287/2021). Study participants were healthy volunteers with no history of malaria or HIV, who had received three doses of either 20 µg (F6–F10) or 40 µg (F1–F5) FMP013 in ALFQ adjuvant on days 1, 29, and 57.

In vitro T cell expansion

PBMCs were thawed and resuspended in 5 ml RPMI containing 10% FCS (U.S. origin), 2 mM glutamine, 1.2% penicillin/streptomycin, and 1.5% 1 M HEPES (expansion medium). Cells were divided into three aliquots, and 1 × 10^6 cells were incubated with the C-CSP or N-CSP peptide pools (15mer peptides, 11aa overlap N-CSP: aa 20–281; C-CSP: aa 271–385) or an equivalent amount of DMSO (unstimulated control), respectively. After incubation for 1 h at 37°C, cells were washed with 5 ml RPMI, combined with 2 × 10^6 unstimulated cells, and seeded into a 48-well cell culture plates at densities of 1.5 × 10^6 cells per well. To provide co-stimulatory signals, 20 U/ml recombinant IL-2 (Stemcell) and 0.5 µg/ml CD28 antibody (BD Biosciences) were added to the culture. On days 4 and 7, the expansion medium was exchanged, and cells were transferred to a 24-well cell culture plate according to the cell density. On day 9, cells were starved for 24 h in medium without IL-2 supplementation to minimize unspecific activation.

Flow cytometry and single-cell sorting

10-day stimulated and expanded cells were incubated for 30 min at 4°C in the dark with 100 µl of antibody staining cocktail containing the following antibodies diluted in FACS buffer (4% FBS in PBS): CD3-FITC (catalog no. 317306; BioLegend), CD4-APC-Cy7 (catalog no. 357416; BioLegend), CD8a-Alexa Fluor 700 (catalog no. 344724; BioLegend), CD137-BV785 (cat. no. 744397; BD Biosciences), CD69-Alexa Fluor647 (catalog no. 310918; BioLegend), OX40-BV421 (cat. no. 350013; BioLegend), and CD25-PE (catalog no. 302606; BioLegend). Freshly thawed and washed PBMCs were incubated for 30 min at 4°C in the dark with 100 µl of antibody staining cocktail containing the following antibodies diluted in FACS buffer: CD3-FITC (catalog no. 317306; BioLegend), CD4-APC-Cy7 (catalog no. 357416; BioLegend), CD8a-Alexa Fluor 700 (catalog no. 344724; BioLegend), CD137-BV785 (catalog no. 744397; BD Biosciences), PD-1-BV605 (catalog no. 329924; BioLegend), CXCR5-Alexa Fluor 647 (catalog no. 558113;

BD Biosciences), ICOS-PE (catalog no. 313520r; BioLegend), CCR7-BV710 (catalog no. 353228; BioLegend), and CD45RA-BV510 (catalog no. 304142; BioLegend). Cells were then washed in FACS buffer and incubated in 100 µl live-dead marker 7-aminoactinomycin D (7AAD) for 10 min at 4°C in the dark. For flow cytometric measurements and index cell sorting, cells were resuspended in FACS buffer at 2 × 10^6 cells per ml. Single $CD8^+7AAD^-CD3^+CCR7^-$ T cells with an activated phenotype based on surface expression of 4-1BB (CD137), PD-1, ICOS, or CXCR5 were isolated from freshly thawed PBMC samples or after 10-day in vitro expansion culture based on a $7AAD^-CD3^+CD4^+$ or $7AAD^-CD3^+CD8^+$ phenotype and high expression of CD25 and OX40 or CD69 and CD137, respectively. Cells were analyzed or isolated using a FACS Aria III (BD). Cells were sorted into 384-well plates using the indexed sort option of the Diva software.

cDNA synthesis and *TR* gene amplification

cDNA synthesis and *TCR* gene amplification were performed as previously described (Wahl et al., 2022a). In brief, cDNA synthesis was performed in the original sort plates using random hexamer primers. *TRA* and *TRB* gene amplification was performed by individual semi-nested PCR using separate *TRAV*- and *TRBV*-specific primer sets. Row- and column-specific barcodes attached to the second PCR primers allowed pooling of all amplicons for next-generation sequencing using Illumina MiSeq or NextSeq 2x300.

TCR sequence analysis

TCR gene sequence analysis and segment annotation were performed using SciReptor (Imkeller et al., 2016; Wahl et al., 2022a). In brief, paired sequencing reads were assembled using PandaSeq setting the maximal and minimal length thresholds to 550 and 300 bp, respectively (Masella et al., 2012), with a minimal overlap of 50 bp and read quality score above 0.8. Reads are assigned to their plate position according to the column- and row-specific barcodes. V, D, and J segments, as well as complementarity-determining region and framework regions, were identified by Ig BLAST and annotated (Ye et al., 2013). Cell phenotype data from index sort fcs files and metadata were linked to the sequence information and stored in a relational MySQL database. Further analysis of the clonal composition and sequence features were performed in R (version 3.4.2) and Rstudio (version 1.3.1093) using the following packages: ggplot2, ggalluvial, pheatmap, vegan, stringr, and dplyr. Clustering of TCR according to sequence similarity was performed using the BLscore package.

TCR expression cloning

TCRs were selected for functional characterization based on a scoring system, including enriched V segment usage, V segment pairing, clone size, and TCR clustering based on BLscore algorithm (Wahl et al., 2022a). TCRs that scored in one or several categories were cloned. The cloning and expression of TCRs in $TCR^{neg}CD3^+CD4^+$ or $TCR^{neg}CD3^+CD8^+$ Jurkat cells (J76-CD4 and J76-CD8) was performed as previously described (Wahl et al., 2022a). In brief, full-length *TRA* and *TRB* genes were cloned into retroviral pMSCV-PlmC expression vectors. If two productive *TRA* genes were detected in one cell, the one with the higher copy number was chosen for cloning. After cloning and sequence verification, Phoenix Ampho cells (American Type Culture Collection, catalog no. CRL-3213; RRID:CVCL_H716) were transfected with the TCR expression vectors using 2.5 M $CaCl_2$ and HEPES-buffered saline and cultured in DMEM GlutaMAX medium (Life Technologies) with 10% heat-inactivated FBS at 37°C and 5% CO_2. Retroviral particles were harvested from the supernatants the next day and used for the transduction of J76-$CD4^+$ and J76-$CD8^+$ T cells. For spin infections, 5 × 10^5 J76 cells were resuspended in 1 ml retroviral supernatant containing 10 µg/ml protamine sulfate, plated in 24-well tissue culture plates, and spun at 2,000 g and 32°C for 1.5 h. Afterward, 1 ml of RPMI 1640 supplemented with 10% heat-inactivated FBS and 2 mM glutamine was added, and cells were incubated for 2 days at 37°C and 5% CO_2. After 7 days of puromycin dihydrochloride (0.8 µg/ml) selection, TCR expression was confirmed by flow cytometric analysis by anti-TCR (catalog no. 306720; BioLegend) and LIVE/DEAD fixable Near-IR dead cell (catalog no. L34975; Invitrogen) staining. Only cell lines with TCR expression levels above 10% TCR^+ cells were screened for reactivity.

TCR reactivity testing

TCR reactivity tests and EBV immortalization were performed as described previously (Wahl et al., 2022a). In brief, 2.13 × 10^5 EBV-immortalized B cells were seeded in 100 µl AIM-V medium into 96-well U-bottom tissue culture plate and loaded with peptide (2.5 µg/ml) for 2–4 h at 37°C and 5% CO_2 before addition of 4.27 × 10^5 TCR-transgenic J76 T cells in 100 µl AIM-V medium. For HLA-blocking experiments, HLA-DR (catalog no. 307602; BioLegend), HLA-DQ (catalog no. 10–4134; Abeomics), HLA-DP (catalog no. H260; Leinco Technologies), HLA-A (catalog no. 36–2474; Abeomics), HLA-B (catalog no. 36–2475 Abeomics), HLA-C (catalog no. 373302; BioLegend), or HLA-E (catalog no. 14–9953-82; Invitrogen)-blocking antibody was added at a concentration of 10 µg/ml together with T cells (Cassotta et al., 2020). After 24 h of incubation at 37°C, supernatants were harvested and serially diluted for IL-2 concentration ELISAs in 384-well plates using one quarter of the recommended reaction volumes for the human IL-2 ELISA MAX Deluxe kit (BioLegend). OD values were measured at 450 nm with a M1000 Pro plate reader (Tecan). IL-2 concentrations were determined and plotted using Excel and GraphPad Prism 9.

HLA typing

For HLA typing, gDNA was extracted from PBMCs using the DNeasy Blood and Tissue Kit (Qiagen) according to the manufacturer's instructions. HLA typing was performed at the Institute for Immunology and Genetics, Kaiserslautern, Germany, or at the DKMS facility, Dresden, Germany.

Peptide MHC in vitro–binding assay

PfCSP peptides covering the major predicted binders identified by NetMHCpan4.0 were loaded onto five MHC monomers (Immudex) and coupled to streptavidin beads (Spherotech) following the instruction provided by Immudex. The level of peptide binding was quantified using a fluorescently labeled

antibody against a conformational epitope within the β2-microglobulin domain, which is only accessible when peptide is bound. For each allele, a positive control peptide provided by Immudex and an empty molecule as negative control were included. Peptide binding was calculated relative to the allele-specific negative control as fold change in median fluorescence intensity and the threshold for binding was set to median fluorescence intensity fold change of 2.

MHC-binding predictions

MHC peptide-binding predictions were performed using the NetMHCpan4.0 algorithm (Reynisson et al., 2020). All 8mer, 9mer, and 10mer peptides covering the FMP013 immunogen sequence (aa 20–380) were included in the analysis and evaluated for binding to HLA-A and HLA-B alleles expressed by at least one of five donors (F1–F5) enrolled in the FMP013 study. All predicted binders (EL-rank <7) were plotted.

Online supplemental material

Fig. S1 shows the gating and isolation strategy of activated $CD4^+$ and $CD8^+$ T cells as well as TCR repertoire and function data. Fig. S2 shows the characterization of TCRs from activated dextramer-reactive $CD8^+$ T cells isolated from in vitro–stimulated PBMC cultures. Table S1 contains the TCR gene sequence information and reactivity data of all TCRs that have been screened in this study.

Data availability

The data underlying Figs. 2, 3, and 4 are available in the published article and its online supplemental material. The data underlying Figs. 1 and 5 are openly available in Zenodo https://doi.org/10.5281/zenodo.14532812.

Acknowledgments

We thank Christine Niesik, Yasmin Bergmann, Julia Gärtner, and Dorien Foster for their experimental assistance, Dr. Christian Busse for his support in data management and technical advice and Dr. Frank Momburg, Dr. Marten Meyer, and Dr. Valerie Oberhardt for their technical input and discussions. We are grateful to Dr. Theresa Kissel and Hendrik Feuerstein for critical reading of the manuscript and thank the vaccine trial participants and all members of the clinical trial unit at Walter Reed for their contribution and commitment to vaccine research. We thank Dr. Elke Bergmann-Leitner and the Walter Reed Army Institute of Research (WRAIR) Immunology Core Facility personnel for processing cells and serum samples from the FMP013 clinical trial. Clinical trial (NCT04268420) was conducted under a WRAIR Institutional Review Board–approved protocol (2651), and the current study was approved by University of Heidelberg Ethics Committee (S-287/2021). The investigators have adhered to the policies for protection of human subjects as prescribed in AR 70–25. The material has been reviewed by the WRAIR. There is no objection to its presentation and/or publication. The opinions or assertions contained herein are the private views of the author and are not to be construed as official or as reflecting true views of the Department of the Army, the Department of Defense.

Open Access funding provided by Deutsches Krebsforschungszentrum in der Helmholtz Gemeinschaft.

Author contributions: H. van Dijk: conceptualization, data curation, formal analysis, investigation, visualization, and writing—original draft, review, and editing. I. Wahl: conceptualization, investigation, methodology, supervision, and writing—review and editing. S. Kraker: investigation and writing—review and editing. P.M. Robben: resources and writing—review and editing. S. Dutta: conceptualization, formal analysis, investigation, methodology, and writing—review and editing. H. Wardemann: conceptualization, funding acquisition, project administration, supervision, and writing—review and editing.

Disclosures: The authors declare no competing interests exist.

Submitted: 6 January 2025
Revised: 31 March 2025
Accepted: 18 June 2025

References

Agnandji, S.T., B. Lell, S.S. Soulanoudjingar, J.F. Fernandes, B.P. Abossolo, C. Conzelmann, B.G.N.O. Methogo, Y. Doucka, A. Flamen, et al. 2011. First results of phase 3 trial of RTS,S/AS01 malaria vaccine in African children. *N. Engl. J. Med.* 365:1863–1875. https://doi.org/10.1056/NEJMoa1102287

Bejon, P., M.T. White, A. Olotu, K. Bojang, J.P.A. Lusingu, N. Salim, N.N. Otsyula, S.T. Agnandji, K.P. Asante, S. Owusu-Agyei, et al. 2013. Efficacy of RTS,S malaria vaccines: Individual-participant pooled analysis of phase 2 data. *Lancet Infect. Dis.* 13:319–327. https://doi.org/10.1016/S1473-3099(13)70005-7

Beura, L.K., S.C. Jameson, and D. Masopust. 2018. Is a human CD8 T-cell vaccine possible, and if so, what would it take? CD8 T-cell vaccines: To B or not to B? *Cold Spring Harb. Perspect. Biol.* 10:a028910. https://doi.org/10.1101/cshperspect.a028910

Burel, J.G., S.H. Apte, P.L. Groves, K. Klein, J.S. McCarthy, and D.L. Doolan. 2016. Reduced Plasmodium Parasite Burden Associates with CD38+ CD4+ T Cells Displaying Cytolytic Potential and Impaired IFN-γ Production. *PloS Pathog.* 12:e1005839. https://doi.org/10.1371/journal.ppat.1005839

Casares, S., T.-D. Brumeanu, and T.L. Richie. 2010. The RTS,S malaria vaccine. *Vaccine*. 28:4880–4894. https://doi.org/10.1016/j.vaccine.2010.05.033

Cassotta, A., P. Paparoditis, R. Geiger, R.R. Mettu, S.J. Landry, A. Donati, M. Benevento, M. Foglierini, D.J.M. Lewis, A. Lanzavecchia, et al. 2020. Deciphering and predicting $CD4^+$ T cell immunodominance of influenza virus hemagglutinin. *J. Exp. Med.* 217:e20200206. https://doi.org/10.1084/jem.20200206

Chronister, W.D., A. Crinklaw, S. Mahajan, R. Vita, Z. Koşaloğlu-Yalçın, Z. Yan, J.A. Greenbaum, L.E. Jessen, M. Nielsen, S. Christley, et al. 2021. TCRMatch: Predicting T-cell receptor specificity based on sequence similarity to previously characterized receptors. *Front. Immunol.* 12:640725. https://doi.org/10.3389/fimmu.2021.640725

Coppi, A., R. Natarajan, G. Pradel, B.L. Bennett, E.R. James, M.A. Roggero, G. Corradin, C. Persson, R. Tewari, and P. Sinnis. 2011. The malaria circumsporozoite protein has two functional domains, each with distinct roles as sporozoites journey from mosquito to mammalian host. *J. Exp. Med.* 208:341–356. https://doi.org/10.1084/jem.20101488

Datoo, M.S., A. Dicko, H. Tinto, J.-B. Ouédraogo, M. Hamaluba, A. Olotu, E. Beaumont, F. Ramos Lopez, H.M. Natama, S. Weston, et al. 2024. Safety and efficacy of malaria vaccine candidate R21/matrix-M in African children: A multicentre, double-blind, randomised, phase 3 trial. *Lancet*. 403:533–544. https://doi.org/10.1016/S0140-6736(23)02511-4

Datoo, M.S., H.M. Natama, A. Somé, D. Bellamy, O. Traoré, T. Rouamba, M.C. Tahita, N.F.A. Ido, P. Yameogo, D. Valia, et al. 2022. Efficacy and immunogenicity of R21/Matrix-M vaccine against clinical malaria after 2 years' follow-up in children in Burkina Faso: A phase 1/2b randomised controlled trial. *Lancet Infect. Dis.* 22:1728–1736. https://doi.org/10.1016/S1473-3099(22)00442-X

Davari, K., T. Holland, L. Prassmayer, G. Longinotti, K.P. Ganley, L.J. Pechilis, I. Diaconu, P.R. Nambiar, M.S. Magee, D.J. Schendel, et al. 2021. Development of a CD8 co-receptor independent T-cell receptor specific for tumor-associated antigen MAGE-A4 for next generation T-cell-based immunotherapy. *J. Immunother. Cancer*. 9:e002035. https://doi.org/10.1136/jitc-2020-002035

de la Cruz, V.F., W.L. Maloy, L.H. Miller, A.A. Lal, M.F. Good, and T.F. McCutchan. 1988. Lack of cross-reactivity between variant T cell determinants from malaria circumsporozoite protein. *J. Immunol.* 141: 2456–2460

Doolan, D.L., S.L. Hoffman, S. Southwood, P.A. Wentworth, J. Sidney, R.W. Chesnut, E. Keogh, E. Appella, T.B. Nutman, A.A. Lal, et al. 1997. Degenerate cytotoxic T cell epitopes from *P. falciparum* restricted by multiple HLA-A and HLA-B supertype alleles. *Immunity*. 7:97–112. https://doi.org/10.1016/s1074-7613(00)80513-0

Doolan, D.L., R.A. Houghten, and M.F. Good. 1991. Location of human cytotoxic T cell epitopes within a polymorphic domain of the *Plasmodium falciparum* circumsporozoite protein. *Int. Immunol.* 3:511–516. https://doi.org/10.1093/intimm/3.6.511

Furtado, R., M. Paul, J. Zhang, J. Sung, P. Karell, K. Ryung S, S. Caillat-Zucman, L. Liang, P. Felgner, et al. 2023. Cytolytic circumsporozoite-specific memory CD4(+) T cell clones are expanded during Plasmodium falciparum infection. *Nat. Commun.* 14:7726. https://doi.org/10.1038/s41467-023-43376-y

Gondré-Lewis, T.A., C. Jiang, M.L. Ford, D.M. Koelle, A. Sette, A.K. Shalek, and P.G. Thomas. 2023. NIAID workshop on T cell technologies. *Nat. Immunol.* 24:14–18. https://doi.org/10.1038/s41590-022-01377-x

González, J.M., K. Peter, F. Esposito, I. Nebié, J.M. Tiercy, A. Bonelo, M. Arévalo-Herrera, D. Valmori, P. Romero, S. Herrera, et al. 2000 HLA-A*0201 restricted CD8⁺ T-lymphocyte responses to malaria: Identification of new *Plasmodium falciparum* epitopes by IFN-gamma ELISPOT. *Parasite Immunol.* 22:501–514. https://doi.org/10.1046/j.1365-3024.2000.00331.x

Good, M.F., W.L. Maloy, M.N. Lunde, H. Margalit, J.L. Cornette, G.L. Smith, B. Moss, L.H. Miller, and J.A. Berzofsky. 1987. Construction of synthetic immunogen: Use of new T-helper epitope on malaria circumsporozoite protein. *Science*. 235:1059–1062. https://doi.org/10.1126/science.2434994

Good, M.F., D. Pombo, I.A. Quakyi, E.M. Riley, R.A. Houghten, A. Menon, D.W. Alling, J.A. Berzofsky, and L.H. Miller. 1988. Human T-cell recognition of the circumsporozoite protein of *Plasmodium falciparum*: Immunodominant T-cell domains map to the polymorphic regions of the molecule. *Proc. Natl. Acad. Sci. USA*. 85:1199–1203. https://doi.org/10.1073/pnas.85.4.1199

Guttinger, M., P. Caspers, B. Takacs, A. Trzeciak, D. Gillessen, J.R. Pink, and F. Sinigaglia. 1988. Human T cells recognize polymorphic and non-polymorphic regions of the *Plasmodium falciparum* circumsporozoite protein. *Embo J.* 7:2555–2558. https://doi.org/10.1002/j.1460-2075.1988.tb03104.x

Hassert, M., S. Arumugam, and J.T. Harty. 2023. Memory CD8⁺ T cell-mediated protection against liver-stage malaria. *Immunol. Rev.* 316: 84–103. https://doi.org/10.1111/imr.13202

Heide, J., K.C. Vaughan, A. Sette, T. Jacobs, and J. Schulze zur Wiesch. 2019. Comprehensive review of human *Plasmodium falciparum*-specific CD8⁺ T cell epitopes. *Front. Immunol.* 10:397. https://doi.org/10.3389/fimmu.2019.00397

Hoffman, S.L., and D.L. Doolan. 2000. Can malaria DNA vaccines on their own be as immunogenic and protective as prime-boost approaches to immunization? *Dev. Biol.* 104:121–132

Hoffman, S.L., D. Isenbarger, G.W. Long, M. Sedegah, A. Szarfman, L. Waters, M.R. Hollingdale, P.H. van der Meide, D.S. Finbloom, and W.R. Ballou. 1989. Sporozoite vaccine induces genetically restricted T cell elimination of malaria from hepatocytes. *Science*. 244:1078–1081. https://doi.org/10.1126/science.2524877

Hutter, J.N., P.M. Robben, C. Lee, M. Hamer, J.E. Moon, K. Merino, L. Zhu, H. Galli, X. Quinn, D.R. Brown, et al. 2022. First-in-human assessment of safety and immunogenicity of low and high doses of *Plasmodium falciparum* malaria protein 013 (FMP013) administered intramuscularly with ALFQ adjuvant in healthy malaria-naïve adults. *Vaccine*. 40: 5781–5790. https://doi.org/10.1016/j.vaccine.2022.08.048

Imkeller, K., P.F. Arndt, H. Wardemann, and C.E. Busse. 2016. sciReptor: analysis of single-cell level immunoglobulin repertoires. *BMC Bioinformatics*. 17:67. https://doi.org/10.1186/s12859-016-0920-1

Lalvani, A., P. Moris, G. Voss, A.A. Pathan, K.E. Kester, R. Brookes, E. Lee, M. Koutsoukos, M. Plebanski, M. Delchambre, et al. 1999. Potent induction of focused Th1-type cellular and humoral immune responses by RTS,S/SBAS2, a recombinant *Plasmodium falciparum* malaria vaccine. *J. Infect. Dis.* 180:1656–1664. https://doi.org/10.1086/315074

Lamers, O.A.C., B.M.D. Franke-Fayard, J.P.R. Koopman, G.V.T. Roozen, J.J. Janse, S.C. Chevalley-Maurel, F.J.A. Geurten, H.M. de Bes-Roeleveld, E. Iliopoulou, E. Colstrup, et al. 2024. Safety and efficacy of immunization with a late-liver-stage attenuated malaria parasite. *N. Engl. J. Med.* 391: 1913–1923. https://doi.org/10.1056/NEJMoa2313892

Laugel, B., H.A. van den Berg, E. Gostick, D.K. Cole, L. Wooldridge, J. Boulter, A. Milicic, D.A. Price, and A.K. Sewell. 2007. Different T cell receptor affinity thresholds and CD8 coreceptor dependence govern cytotoxic T lymphocyte activation and tetramer binding properties. *J. Biol. Chem.* 282:23799–23810. https://doi.org/10.1074/jbc.M700976200

Masella, A.P., A.K. Bartram, J.M. Truszkowski, D.G. Brown, and J.D. Neufeld. 2012. PANDAseq: Paired-end assembler for illumina sequences. *BMC Bioinformatics*. 13:31. https://doi.org/10.1186/1471-2105-13-31

Montes, M., N. Rufer, V. Appay, S. Reynard, M.J. Pittet, D.E. Speiser, P. Guillaume, J.-C. Cerottini, P. Romero, and S. Leyvraz. 2005. Optimum in vitro expansion of human antigen-specific CD8 T cells for adoptive transfer therapy. *Clin. Exp. Immunol.* 142:292–302. https://doi.org/10.1111/j.1365-2249.2005.02914.x

Moreno, A., P. Clavijo, R. Edelman, J. Davis, M. Sztein, D. Herrington, and E. Nardin. 1991. Cytotoxic CD4⁺ T cells from a sporozoite-immunized volunteer recognize the *Plasmodium falciparum* CS protein. *Int. Immunol.* 3:997–1003. https://doi.org/10.1093/intimm/3.10.997

Moreno, A., P. Clavijo, R. Edelman, J. Davis, M. Sztein, F. Sinigaglia, and E. Nardin. 1993. CD4⁺ T cell clones obtained from *Plasmodium falciparum* sporozoite-immunized volunteers recognize polymorphic sequences of the circumsporozoite protein. *J. Immunol.* 151:489–499

Nardin, E. H., D. A. Herrington, J. Davis, M. Levine, D. Stuber, B. Takacs, P. Caspers, P. Barr, R. Altszuler, P. Clavijo, et al. 1989. Conserved repetitive epitope recognized by CD4+ clones from a malaria-immunized volunteer. *Science*. 246:1603–1606. https://doi.org/10.1126/science.2480642

Neafsey, D.E., M. Juraska, T. Bedford, D. Benkeser, C. Valim, A. Griggs, M. Lievens, S. Abdulla, S. Adjei, T. Agbenyega, et al. 2015. Genetic diversity and protective efficacy of the RTS,S/AS01 malaria vaccine. *N. Engl. J. Med.* 373:2025–2037. https://doi.org/10.1056/NEJMoa1505819

Oberhardt, V., H. Luxenburger, J. Kemming, I. Schulien, K. Ciminski, S. Giese, B. Csernalabics, J. Lang-Meli, I. Janowska, J. Staniek, et al. 2021. Rapid and stable mobilization of CD8⁺ T cells by SARS-CoV-2 mRNA vaccine. *Nature*. 597:268–273. https://doi.org/10.1038/s41586-021-03841-4

Oliveira, G.A., K.A. Kumar, J.M. Calvo-Calle, C. Othoro, D. Altszuler, V. Nussenzweig, and E.H. Nardin. 2008. Class II-restricted protective immunity induced by malaria sporozoites. *Infect. Immun.* 76:1200–1206. https://doi.org/10.1128/IAI.00566-07

Pallikkuth, S., S. Chaudhury, P. Lu, L. Pan, E. Jongert, U. Wille-Reece, and S. Pahwa. 2020. A delayed fractionated dose RTS,S AS01 vaccine regimen mediates protection via improved T follicular helper and B cell responses. *Elife*. 9:e51889. https://doi.org/10.7554/eLife.51889

Reece, W.H.H., M. Pinder, P.K. Gothard, P. Milligan, K. Bojang, T. Doherty, M. Plebanski, P. Akinwunmi, S. Everaere, K.R. Watkins, et al. 2004. A CD4(+) T-cell immune response to a conserved epitope in the circumsporozoite protein correlates with protection from natural *Plasmodium falciparum* infection and disease. *Nat. Med.* 10:406–410. https://doi.org/10.1038/nm1009

Reiss, S., A.E. Baxter, K.M. Cirelli, J.M. Dan, A. Morou, A. Daigneault, N. Brassard, G. Silvestri, J.-P. Routy, C. Havenar-Daughton, et al. 2017. Comparative analysis of activation induced marker (AIM) assays for sensitive identification of antigen-specific CD4 T cells. *PLoS One*. 12: e0186998. https://doi.org/10.1371/journal.pone.0186998

Rénia, L., D. Grillot, M. Marussig, G. Corradin, F. Miltgen, P.H. Lambert, D. Mazier, and G. Del Giudice. 1993. Effector functions of circumsporozoite peptide-primed CD4⁺ T cell clones against *Plasmodium yoelii* liver stages. *J. Immunol.* 150:1471–1478

Rénia, L., M.S. Marussig, D. Grillot, S. Pied, G. Corradin, F. Miltgen, G. Del Giudice, and D. Mazier. 1991. In vitro activity of CD4⁺ and CD8⁺ T lymphocytes from mice immunized with a synthetic malaria peptide. *Proc. Natl. Acad. Sci. USA*. 88:7963–7967. https://doi.org/10.1073/pnas.88.18.7963

Reynisson, B., B. Alvarez, S. Paul, B. Peters, and M. Nielsen. 2020. NetMHCpan-4.1 and NetMHCIIpan-4.0: Improved predictions of MHC antigen presentation by concurrent motif deconvolution and integration of MS MHC eluted ligand data. *Nucl. Acids Res.* 48:W449–W454. https://doi.org/10.1093/nar/gkaa379

Rodrigues, M.M., A.-S. Cordey, G. Arreaza, G. Corradin, P. Romero, J.L. Maryanski, R.S. Nussenzweig, and F. Zavala. 1991. CD8⁺ cytolytic T cell

clones derived against the *Plasmodium yoelii* circumsporozoite protein protect against malaria. *Int. Immunol.* 3:579–585. https://doi.org/10.1093/intimm/3.6.579

Romero, P., J.L. Maryanski, G. Corradin, R.S. Nussenzweig, V. Nussenzweig, and F. Zavala. 1989. Cloned cytotoxic T cells recognize an epitope in the circumsporozoite protein and protect against malaria. *Nature*. 341: 323–326. https://doi.org/10.1038/341323a0

RTS,S Clinical Trials Partnership. 2014. Efficacy and safety of the RTS,S/AS01 malaria vaccine during 18 months after vaccination: A phase 3 randomized, controlled trial in children and young infants at 11 African sites. *PLoS Med.* 11:e1001685. https://doi.org/10.1371/journal.pmed.1001685

Schofield, L., J. Villaquiran, A. Ferreira, H. Schellekens, R. Nussenzweig, and V. Nussenzweig. 1987. γ Interferon, $CD8^+$ T cells and antibodies required for immunity to malaria sporozoites. *Nature*. 330:664–666. https://doi.org/10.1038/330664a0

Schwenk, R., J.M. Lumsden, L.E. Rein, L. Juompan, K.E. Kester, D.G. Heppner, and U. Krzych. 2011. Immunization with the RTS,S/AS malaria vaccine induces IFN-γ(+)CD4 T cells that recognize only discrete regions of the circumsporozoite protein and these specificities are maintained following booster immunizations and challenge. *Vaccine*. 29:8847–8854. https://doi.org/10.1016/j.vaccine.2011.09.098

Sedegah, M., Y. Kim, H. Ganeshan, J. Huang, M. Belmonte, E. Abot, J.G. Banania, F. Farooq, S. McGrath, B. Peters, et al. 2013. Identification of minimal human MHC-restricted $CD8^+$ T-cell epitopes within the *Plasmodium falciparum* circumsporozoite protein (CSP). *Malar. J.* 12:185. https://doi.org/10.1186/1475-2875-12-185

Seder, R.A., L.-J. Chang, M.E. Enama, K.L. Zephir, U.N. Sarwar, I.J. Gordon, L.A. Holman, E.R. James, P.F. Billingsley, A. Gunasekera, et al. 2013. Protection against malaria by intravenous immunization with a nonreplicating sporozoite vaccine. *Science*. 341:1359–1365. https://doi.org/10.1126/science.1241800

Singer, M., S. Kanatani, S.G. Castillo, F. Frischknecht, and P. Sinnis. 2024. The *Plasmodium* circumsporozoite protein. *Trends Parasitol.* 40:1124–1134. https://doi.org/10.1016/j.pt.2024.10.017

Sinigaglia, F., M. Guttinger, D. Gillessen, D.M. Doran, B. Takacs, H. Matile, A. Trzeciak, and J.R. Pink. 1988a. Epitopes recognized by human T lymphocytes on malaria circumsporozoite protein. *Eur. J. Immunol.* 18: 633–636. https://doi.org/10.1002/eji.1830180422

Sinigaglia, F., M. Guttinger, J. Kilgus, D.M. Doran, H. Matile, H. Etlinger, A. Trzeciak, D. Gillessen, and J.R. Pink. 1988b. A malaria T-cell epitope recognized in association with most mouse and human MHC class II molecules. *Nature*. 336:778–780. https://doi.org/10.1038/336778a0

Tanabe, K., T. Mita, N.M.Q. Palacpac, N. Arisue, T. Tougan, S. Kawai, T. Jombart, F. Kobayashi, and T. Horii. 2013. Within-population genetic diversity of *Plasmodium falciparum* vaccine candidate antigens reveals geographic distance from a Central sub-Saharan African origin. *Vaccine*. 31:1334–1339. https://doi.org/10.1016/j.vaccine.2012.12.039

Trimnell, A., A. Takagi, M. Gupta, T.L. Richie, S.H. Kappe, and R. Wang. 2009. Genetically attenuated parasite vaccines induce contact-dependent $CD8^+$ T cell killing of *Plasmodium yoelii* liver stage-infected hepatocytes. *J. Immunol.* 183:5870–5878. https://doi.org/10.4049/jimmunol.0900302

Tsuji, M., and F. Zavala. 2001. Peptide-based subunit vaccines against preerythrocytic stages of malaria parasites. *Mol. Immunol.* 38:433–442. https://doi.org/10.1016/s0161-5890(01)00079-7

Wahl, I., S. Hoffmann, R. Hundsdorfer, J. Puchan, S.L. Hoffman, P.G. Kremsner, B. Mordmüller, C.E. Busse, and H. Wardemann. 2022a. An efficient single-cell based method for linking human T cell phenotype to T cell receptor sequence and specificity. *Eur. J. Immunol.* 52:237–246. https://doi.org/10.1002/eji.202149392

Wahl, I., A.S. Obraztsova, J. Puchan, R. Hundsdorfer, S. Chakravarty, B.K.L. Sim, S.L. Hoffman, P.G. Kremsner, B. Mordmüller, and H. Wardemann. 2022b. Clonal evolution and TCR specificity of the human T_{FH} cell response to *Plasmodium falciparum* CSP. *Sci. Immunol.* 7:eabm9644. https://doi.org/10.1126/sciimmunol.abm9644

Wang, R., D.L. Doolan, T.P. Le, R.C. Hedstrom, K.M. Coonan, Y. Charoenvit, T.R. Jones, P. Hobart, M. Margalith, J. Ng, et al. 1998. Induction of antigen-specific cytotoxic T lymphocytes in humans by a malaria DNA vaccine. *Science*. 282:476–480. https://doi.org/10.1126/science.282.5388.476

Weiss, W.R., and C.G. Jiang. 2012. Protective $CD8^+$ T lymphocytes in primates immunized with malaria sporozoites. *PLoS One*. 7:e31247. https://doi.org/10.1371/journal.pone.0031247

Weiss, W.R., M. Sedegah, R.L. Beaudoin, L.H. Miller, and M.F. Good. 1988. CD8+ T cells (cytotoxic/suppressors) are required for protection in mice immunized with malaria sporozoites. *Proc. Nat. Acad. Sci. USA*. 85: 573–576. https://doi.org/10.1073/pnas.85.2.573

Weiss, W.R., M. Sedegah, J.A. Berzofsky, and S.L. Hoffman. 1993. The role of $CD4^+$ T cells in immunity to malaria sporozoites. *J. Immunol.* 151: 2690–2698

Ye, J., N. Ma, T.L. Madden, and J.M. Ostell. 2013. IgBLAST: An immunoglobulin variable domain sequence analysis tool. *Nucl. Acids Res.* 41: W34–W40. https://doi.org/10.1093/nar/gkt382

Zeeshan, M., M.T. Alam, S. Vinayak, H. Bora, R.K. Tyagi, M.S. Alam, V. Choudhary, P. Mittra, V. Lumb, P.K. Bharti, et al. 2012. Genetic variation in the *Plasmodium falciparum* circumsporozoite protein in India and its relevance to RTS,S malaria vaccine. *PLoS One*. 7:e43430. https://doi.org/10.1371/journal.pone.0043430

JEM

Supplemental material

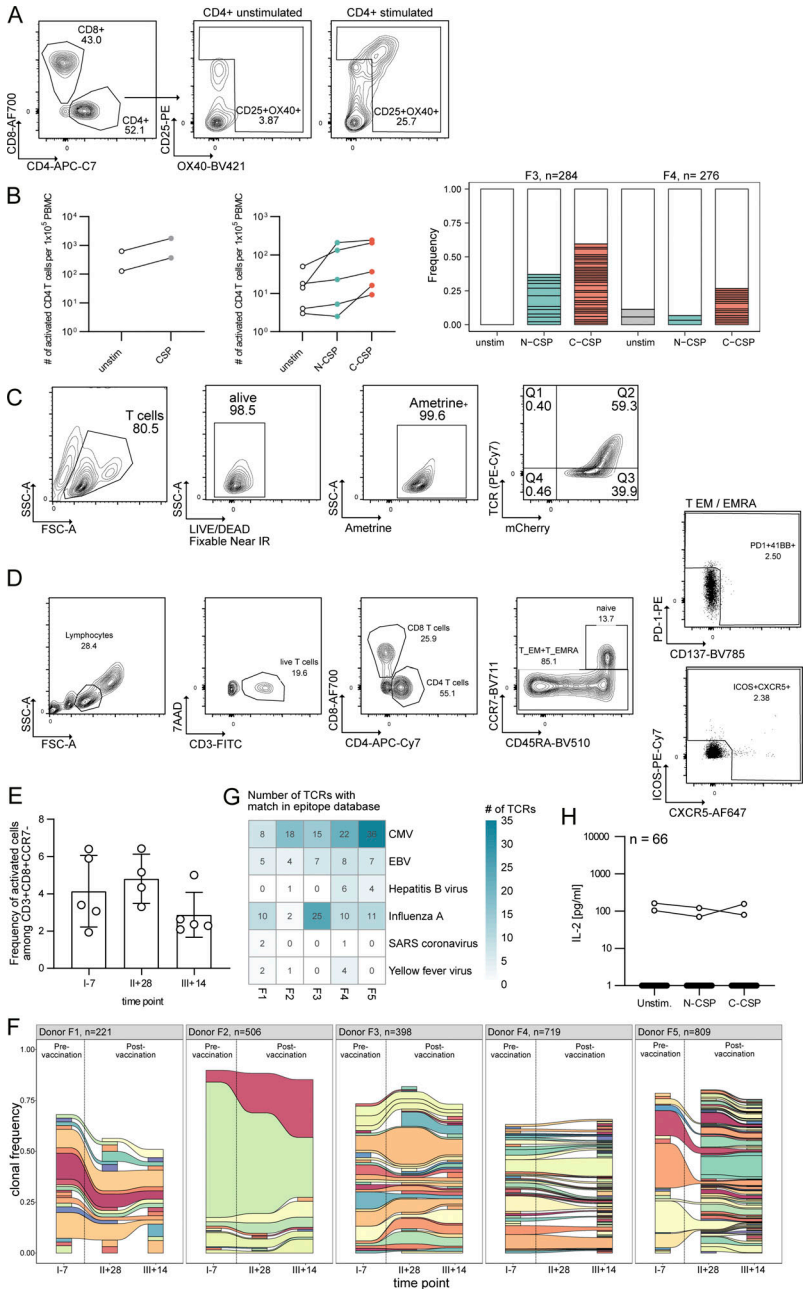

Figure S1. **Gating and isolation strategy of activated CD4⁺ and CD8⁺ T cells and TCR analysis. (A)** Gating strategy of activated CD4⁺ T cells ($CD3^+CD4^+OX40^+CD25^+$) pre-gated on viable ($7AAD^-$) lymphocytes (SSC/FSC) after in vitro stimulation with PfCSP peptides or in unstimulated control culture. **(B)** Left: Number of activated ($CD25^+OX40^+$) CD4⁺ T cells after in vitro PfCSP peptide pool stimulation compared with unstimulated control cells from the same individuals. Each symbol represents a volunteer. Right: Clonal composition of single activated CD4⁺ T cells after N-CSP or C-CSP peptide pool stimulation or unstimulated samples from the indicated donors. Individual expanded clones are shown in color, and all non-expanded clones are shown in white. **(C)** Gating strategy of TCR-transgenic Jurkat76 cell lines based on mCherry ($mCherry^+$) and TCR (TCR^+) expression quantified by flow cytometric analysis. **(D)** Gating strategy for flow cytometric analysis of CD8⁺ T effector memory (T_{EM}) cells or terminally differentiated T_{EM} re-expressing CD45RA (T_{EMRA}) cells in PBMC samples from FMP013/ALFQ vaccinees. **(E)** Frequency of activated ($PD1^+CD137^+ICOS^+CXCR5^+$) T_{EM} or T_{EMRA} cells as frequency of $CD3^+CD8^+CCR7^-$ T cells for five donors (F1–5). Bar plots of individual time points before first (I–7), after second (II+28), and after third (III+14) vaccine dose show mean and standard deviation, with individual dots representing individual donors. **(F)** Activated CD8⁺ $T_{EM+EMRA}$ cells were indexed single-cell sorted, and *TR* genes were amplified and sequenced for subsequent repertoire analysis. Clonal composition of the TCR gene repertoire in individual donors across multiple blood collection time points. Expanded clones are shown in color, while unique TCR sequences are combined in the white compartment. Same color within each donor represents the same clone, while color sharing across different donors does not. **(G)** Number of TCRs with TCR beta chain match in the Immune Epitope Database identified by TCRmatch tool (Chronister et al., 2021). Identified TCRs are stratified by donor (F1–F5) and origin of the target epitope. SARS: severe acute respiratory syndrome. **(H)** Transgenic CD8⁺ Jurkat76 T cell lines expressing TCRs from T cell clones without TCR sequence features of common virus-specific TCRs or presence before vaccination were generated. IL-2 concentrations in supernatants of 67 TCR-transgenic CD8⁺ Jurkat76 T cells co-cultured with autologous B cells pulsed with N-CSP or C-CSP peptide pools or with non-peptide–pulsed autologous B cells (unstimulated control). Data in A–G are from one experiment. **(H)** Data represent one out of two independent experiments.

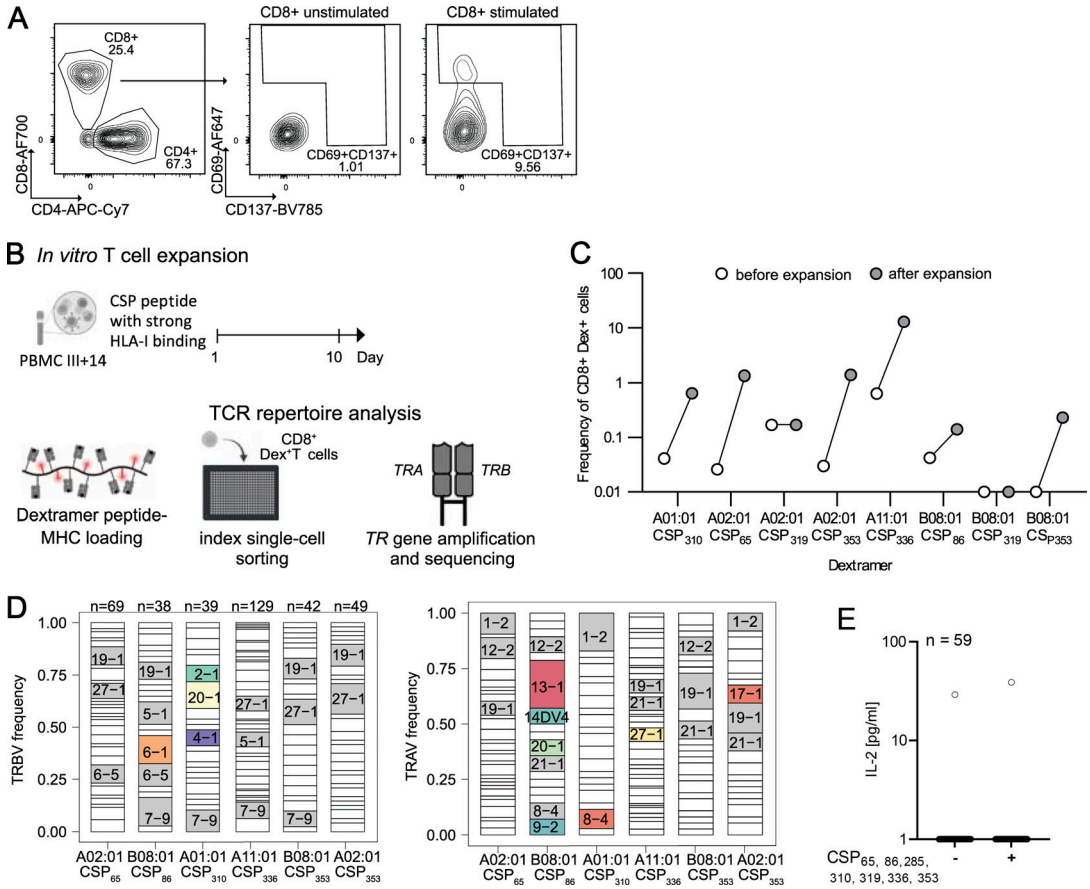

Figure S2. **Isolation and TCR characterization of dextramer-reactive CD8⁺ T cells. (A)** Gating strategy of activated CD8⁺ T cells ($CD3^+CD8^+CD137^+CD69^+$) pre-gated on viable ($7AAD^-$) lymphocytes (SSC/FSC) after in vitro stimulation with PfCSP peptides or in unstimulated control culture. **(B)** Schematic overview of the in vitro stimulation and dextramer-based single-cell isolation strategy. PBMC samples collected 14 days after the third rCSP/ALFQ vaccine dose (III+14) were stimulated with seven CSP peptides and cultured for 10 days. CSP peptide-loaded MHC molecules were bound to dextramer backbone and used for flow cytometry staining of PBMC samples before and after in vitro stimulation. After the stimulation, dextramer⁺ cells were isolated by indexed flow cytometric single-cell sorting for paired *TRA* and *TRB* gene amplification and sequencing. **(C)** Frequency of dextramer⁺ CD8⁺ T cells before and after in vitro stimulation. **(D)** *TRBV* and *TRAV* gene segment usage among dextramer-binding CD8⁺ T cell clones. **(E)** Transgenic CD8⁺ Jurkat76 T cell lines were generated expressing TCRs of dextramer⁺ T cell clones and co-cultured with peptide-pulsed autologous B cells (pulsed with seven predicted CSP peptides) or unstimulated control (non-peptide–pulsed autologous B cells). Il-2 concentration in supernatants. A, C, and D represent data from one experiment. **(E)** One representative out of two independent experiments is shown.

Provided online is Table S1. Table S1 contains the TCR gene sequence information and reactivity data of all TCRs that have been screened in this study.